Low-Complexity Joint Range and Velocity Estimation for OFDM-Based Integrated Sensing and Communication

1st Yuang Cao
School of Information and Electronics
Beijing Institute of Technology
Beijing, China
yuang_cao@bit.edu.cn

2nd Dongxuan He
School of Information and Electronics
Beijing Institute of Technology
Beijing, China
dongxuan_he@bit.edu.cn

3rd Tiancheng Yang
School of Information and Electronics
Beijing Institute of Technology
Beijing, China
tiancheng_yang@bit.edu.cn

4th Hua Wang
School of Information and Electronics
Beijing Institute of Technology
Beijing, China
wanghua@bit.edu.cn

5th Rongkun Jiang
School of Integrated Circuits and Electronics
Beijing Institute of Technology
Beijing, China
jiangrongkun@bit.edu.cn

2025 International Wireless Communications and Mobile Computing (IWCMC) | 979-8-3315-0887-6/25/$31.00 ©2025 IEEE | DOI: 10.1109/IWCMC65282.2025.11059561

***Abstract*—Integrated sensing and communication (ISAC) can realize communication and sensing functionalities simultaneously by sharing spectrum and hardware resources, where the sensing performance can be guaranteed by accurate range and velocity estimation. However joint range and velocity estimation inherently confronts the accuracy-complexity tradeoff. Therefore, a low-complexity joint range and velocity estimation algorithm is developed in this work, referred to as the particle swarm optimization reconstructed subspace multiple signal classification (PSO-RS-MUSIC). The proposed algorithm leverages optimized subspace reuse mechanisms to enhance estimation accuracy. To address the high complexity problem, the PSO-RS-MUSIC algorithm employs the particle swarm optimization (PSO) technique to replace the traditional spectral peak search, thereby reducing computational complexity significantly. Simulation results illustrate that the proposed algorithm outperforms the conventional RS-MUSIC algorithm, while the computational complexity is reduced by more than 90%.**

***Index Terms*—ISAC, PSO-RS-MUSIC, joint range and velocity estimation.**

I. Introduction

Integrated sensing and communication (ISAC) enables simultaneous communication and sensing by sharing a common set of devices and equipment, effectively reducing equipment costs, size, and power consumption, which has become a mainstream development trend for the upcoming sixth generation (6G) mobile communication [1]–[3]. Considering its shared devices and spectrum resource, ISAC systems need to select a appropriate waveform that can efficiently carry communication data while also provide precise sensing capabilities. Hereby, multi-carrier waveforms have emerged as promising candidates for ISAC systems due to their advantages in terms of communication and sensing [4]. For example, orthogonal frequency division multiplexing (OFDM) signals are widely adopted in such systems owing to their notable advantages [5]. For communication, OFDM can achieve high spectral efficiency within given bandwidth through orthogonal subcarrier multiplexing. Furthermore, its capability to mitigate multipath interference can enhance communication reliability, particularly in complex wireless environments. For sensing, OFDM signals can be well compatible with high-range resolution radar applications due to its wide bandwidth. Moreover, the inherent characteristics of OFDM such as ambiguity functions lead to resembling thumbtacks and strong tolerance to Doppler shifts [6].

The development of effective signal-processing algorithms has enabled accurate parameter estimation for sensing echo in OFDM-based ISAC system, which mainly include traditional frequency-domain analysis algorithms such as discrete fourier transform (DFT), array signal processing algorithms such as estimation of signal parameters via rotational invariance techniques (ESPRIT) and multiple signal classification (MUSIC), and statistical estimation algorithms such as maximum likelihood (ML) and least squares (LS) [7]–[9]. Specifically, the DFT algorithm extracts target range and velocity information in frequency-domain, which is efficient but resolution-limited. ESPRIT and MUSIC leverage the separation characteristics of signal and noise subspaces, enabling high-resolution parameter estimation. ML and LS can achieve accurate estimation in complex noise environments based on the statistical optimization criteria. However, these conventional algorithms often exhibit a fundamental trade-off between prohibitive computational complexity and performance. To this end, several new algorithms have been proposed in recent years to compensate for the shortcomings of the conventional methods [10], [11]. The authors in [10] proposed a least square weighted algorithm for integrated radar-communications systems, achieving joint range-velocity estimation through separate dimension search optimization to significantly reduce computational complexity. An improved version of the MUSIC algorithm was introduced to address the rank deficiency issue in parameter estimation, enabling the joint estimation of both angle and range [11].

With the rapid development of signal processing, modern techniques such as intelligent optimization algorithms, compressed sensing, and deep neural networks have been proposed to improve the parameter estimation performance in ISAC system. Among these, various swarm intelligence optimization algorithms can effectively exploit the shape of spatial spectrum functions, eliminating the need for spectrum peak searching and thus reducing computational complexity [12], [13]. The

Authorized licensed use limited to: BEIJING INSTITUTE OF TECHNOLOGY. Downloaded on July 09,2025 at 06:22:15 UTC from IEEE Xplore. Restrictions apply.

authors in [12] combined the classical algorithms, which include MVDR, MUSIC, and ESPRIT, with the optimization algorithms such as particle swarm optimization (PSO) and genetic algorithm (GA) to conduct performance analysis and evaluation. In [13], a deep-augmented MUSIC (DA-MUSIC) algorithm was proposed to enhance the performance and robustness of the MUSIC algorithm. However, these methods suffer from excessively high computational complexity and inadequate real-time processing capability, which fundamentally limit their deployment in practical latency-sensitive ISAC applications.

Against this background, a PSO-RS-MUSIC algorithm is proposed in this paper to reduce the prohibitive computational complexity of conventional spectral peak search in joint range and velocity estimation. By integrating particle swarm optimization (PSO) with subspace reconstruction mechanisms, the algorithm achieves over 90% complexity reduction compared to standard RS-MUSIC while maintaining equivalent estimation accuracy, enabling real-time parameter extraction in resource-constrained ISAC systems.

Notations: Scalars, vectors and matrices are denoted by lowercase letters, lowercase boldface letters, and uppercase boldface letters, respectively. The Kronecker product is denoted by $\otimes$. $\mathbf{I}_N$ is the $N \times N$ identity matrix. $\mathrm{diag}\{\cdot\}$ is a diagonal matrix formed from the components of a vector. The transpose and Hermitian transpose of matrix $\mathbf{A}$ are denoted by $\mathbf{A}^T$ and $\mathbf{A}^H$, respectively.

II. System Model

As shown in Fig. 1, an OFDM ISAC system is considered, where a dual-functional ISAC base station (BS) equipped with two single antennas simultaneously performs downlink multi-user communication and point target radar detection.

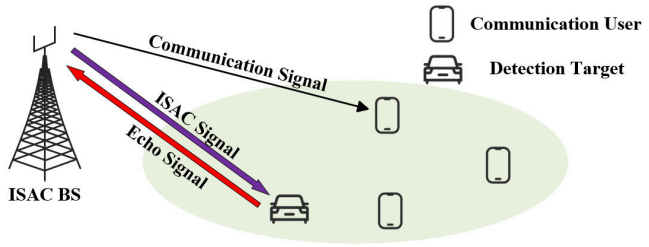

Fig. 1: An illustration of the considered ISAC system.

An OFDM signal is a series of complex modulated signals distributed to each orthogonal subcarrier, and the time domain signal of OFDM can be expressed as

$$x(t) = \sum_{m=0}^{N_s-1} \sum_{n=0}^{N_c-1} c(n,m) e^{j2\pi n \Delta f (t - mT_s)} \times e^{-j2\pi n \Delta f T_{cp}} \mathrm{rect}\left(\frac{t - mT_s}{T_s}\right), \quad (1)$$

where N_s is the number of symbols and N_c is the number of subcarriers, $c(n,m)$ is the communication modulated information and Δf is the frequency interval between adjacent subcarriers. T_s is the duration of a complete OFDM symbol and $T_s = T_{cp} + T$, where T_{cp} is the duration of the cyclic prefix. T is the duration of an OFDM symbol and $T = 1/\Delta f$. The window function $\mathrm{rect}(\cdot)$ is given by

$$\mathrm{rect}\left(\frac{t}{T_s}\right) = \begin{cases} 1, & t \in [0, T_s], \\ 0, & \text{otherwise.} \end{cases} \quad (2)$$

The transmitted signal obtained by upconverting the baseband OFDM signal can be expressed as

$$\widetilde{x}(t) = e^{j2\pi f_c t} x(t), \quad (3)$$

where f_c is the carrier frequency.

From the perspective of radar sensing, the ISAC system achieves range and velocity estimation of point targets by processing the received radar echo signals. Assuming there are K detection targets and the transmission signal is reflected by the k-th target and back to the reception antenna. The signal propagation must account for time delay and Doppler shift effects. Therefore, the echo signal from the k-th target received by the ISAC base station (BS) can be expressed as

$$\widetilde{y}_k(t) = \rho_k \widetilde{x}(t - \tau_k) e^{j2\pi f_{v,k}} + n(t), \quad (4)$$

where ρ_k is the attenuation factor of the echo signal from the k-th target, which is related to the radar cross section and the range between the k-th target and the receiver antenna. The time delay can be expressed as $\tau_k = \frac{2d_k}{c}$, where d_k is the range between the receiver antenna antenna and the k-th target. c is the velocity of light in free space and doppler frequency shift can be expressed as $f_{v,k} = \frac{2v_k f_c}{c}$. The additive white Gaussian noise (AWGN) can be expressed as $n(t) \sim \mathcal{N}(0, \sigma^2)$, where σ^2 is the variance of the noise. Therefore, the echo signal obtained by superimposing the echoes from K targets can be expressed as

$$\widetilde{y}(t) = \sum_{k=1}^{K} \rho_k \widetilde{x}(t - \tau_k) e^{j2\pi f_{v,k}} + n(t). \quad (5)$$

The received signal is down-converted to baseband and followed by sampling and cyclic prefix (CP) removal. Therefore, the discrete-time representation of the radar received signal can be expressed as

$$\mathbf{Y}_{m,n} = \sum_{k=1}^{K} \rho_k \mathbf{C}_{m,n} e^{-j2\pi n \Delta f \tau_k} e^{j2\pi f_{d_k} m T_s} + \mathbf{w}(\mathbf{m}, \mathbf{n}), \quad (6)$$

where $\mathbf{C}_{m,n}$ and $\mathbf{w}(\mathbf{m}, \mathbf{n})$ represent the transmitted modulation signal and AWGN, respectively. Additionally, $\mathbf{C}_{m,n}$ can be removed because it is already known at the receiver. Therefore, Eq. (6) can be expressed as

$$\mathbf{Z}_{m,n} = \sum_{k=1}^{K} \rho_k e^{-j2\pi n \Delta f \tau_k} e^{j2\pi f_{d_k} m T_s} + \mathbf{w}(\mathbf{m}, \mathbf{n}), \quad (7)$$

with $\mathbf{Z}_{m,n} \in \mathbb{C}^{N_c \times N_s}$.

Authorized licensed use limited to: BEIJING INSTITUTE OF TECHNOLOGY. Downloaded on July 09,2025 at 06:22:15 UTC from IEEE Xplore. Restrictions apply.

III. PSO-RS-MUSIC ALGORITHM FOR RANGE-VELOCITY ESTIMATION

A. Subspace Construction

The received signal matrix $\mathbf{Z}_{m,n}$ reveals that its columns exclusively contain range information, whereas rows solely contain velocity information. This inherent structural decoupling fundamentally prohibits direct joint range-velocity estimation through conventional matrix processing techniques. To address this, the received signal matrix $\mathbf{Z}_{m,n}$ can be reshaped into a column vector, which ensures the inclusion of both range and velocity information. However, such reconstruction results in a covariance matrix with a rank of 1, limiting its application to single-target estimation and dimensional inflation in multi-target parameter vectors. To overcome these limitations, a smoothing operation is applied to partition the received signal matrix, enabling joint range-velocity estimation through subspace decoupling and eigenvalue reconstruction.

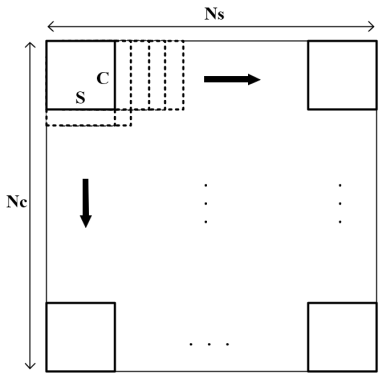

Fig. 2: Illustration of signal matrix segmentation.

The segmentation of the received signal matrix is shown in Fig.2. The signal matrix is first divided into multiple smaller matrices with a size of $C \times S$. Each segmented matrix is then reshaped into a column vector, which represents a single sample of data. Therefore, the entire matrix is formed as a combination of multiple samples, and the dimension of each column vector depends on the size of the segmented matrix, while the number of samples corresponds to the number of segmented matrices.

The segmentation process starts from the first row and shifts to the right. When it reaches the far-right end, it moves to the next row and continues shifting to the right. Following this procedure, the entire matrix is segmented. The first sub-matrix can be expressed as

$$\mathbf{F}_{c,s} = \begin{bmatrix} z_{c-1,s-1} & \cdots & z_{c-1,s+S-1} \\ z_{c,s-1} & \cdots & z_{c,s+S-1} \\ \vdots & \ddots & \vdots \\ z_{c+C-1,s-1} & \cdots & z_{c+C-1,s+S-1} \end{bmatrix}. \tag{8}$$

Each column of the submatrix is concatenated, and the submatrix is subsequently reshaped into a single column vector given by

$$\tilde{\mathbf{F}}_{c,s} = vec(\mathbf{F}_{c,s}), \tag{9}$$

where $ves(\cdot)$ represents the process of reshaping the submatrix into a column vector by concatenating each column into a single long column vector.

After processing the signal matrix, it is necessary to construct its corresponding manifold matrix. To achieve joint range-velocity estimation utilizing the MUSIC algorithm, each element of the manifold matrix must contain both range and velocity information. The velocity-independent and range-independent manifold matrices can be separately defined as follows

$$\begin{aligned} \mathbf{a}_d(\tau) &= \left[1, e^{-j2\pi\Delta f\tau}, \ldots, e^{-j(C-1)2\pi\Delta f\tau}\right]^T, \\ \mathbf{a}_v(f_d) &= \left[1, e^{j2\pi T_s f_d}, \ldots, e^{j(S-1)2\pi T_s f_d}\right]^T. \end{aligned} \tag{10}$$

Based on the one-dimensional manifold matrices for range and velocity estimation, the two-dimensional joint manifold matrix for range and velocity can be expressed as

$$\mathbf{a}(\tau, f_d) = \mathbf{a}_d(\tau) \otimes \mathbf{a}_v(f_d) \in \mathbb{C}^{CS\times 1}, \tag{11}$$

where the single parameter τ and f_d have been extended to the two-dimensional joint parameter (τ, f_d).

B. Conventional RS-MUSIC Algorithm

The joint range and velocity estimation based on the RS-MUSIC algorithm can be performed after completing the receiver matrix segmentation and the construction of the flow matrix. The RS algorithm is based on the eigenvector space of the signal matrix. According to the size of the eigenvalue, the eigenvectors corresponding to the largest signal eigenvalue are eliminated in turn to form a reconstructed subspace to reduce the interference of larger signal characteristic components on the remaining signals. The reconstructed subspace is corrected according to the size of the eigenvalue to form a new set of spatial estimation spectra.

First, the signal and noise subspaces are obtained by performing subspace decomposition on the autocorrelation matrix of the reconstructed signal Y, given by

$$\mathbf{R}_d = \frac{1}{N_p} \sum_{c=1}^{N_c-C+1} \sum_{s=1}^{N_s-S+1} \tilde{\mathbf{F}}_{c,s} \tilde{\mathbf{F}}_{c,s}^H, \tag{12}$$

where $N_p = (N_c - C + 1)(N_s - S + 1)$.

The eigen-decomposition of the autocorrelation matrix yields the eigenvector space and the eigenvalue diagonal matrix, denoted as

$$\mathbf{R}_d = \mathbf{U}^H \mathbf{\Sigma} \mathbf{U}, \tag{13}$$

where $\mathbf{U} = \left[\mathbf{w}_1, \mathbf{w}_2, \cdots, \mathbf{w}_{CS}\right]$ and $\mathbf{\Sigma} = \operatorname{diag}\left[\lambda_1, \lambda_2, \cdots, \lambda_{CS}\right]$.

Based on the magnitude of the eigenvalues, the space can be divided into the signal subspace and the noise subspace, represented as

$$\begin{aligned} \mathbf{U}_S &= \left[\mathbf{w}_1 \quad \mathbf{w}_2 \quad \cdots \quad \mathbf{w}_K\right], \\ \mathbf{U}_N &= \left[\mathbf{w}_{K+1} \quad \mathbf{w}_{K+2} \quad \cdots \quad \mathbf{w}_{CS}\right], \\ \mathbf{\Sigma}_S &= \operatorname{diag}\left[\lambda_1, \lambda_2, \cdots, \lambda_K\right], \\ \mathbf{\Sigma}_N &= \operatorname{diag}\left[\lambda_{K+1}, \lambda_{K+2}, \cdots, \lambda_{CS}\right]. \end{aligned} \tag{14}$$

Authorized licensed use limited to: BEIJING INSTITUTE OF TECHNOLOGY. Downloaded on July 09,2025 at 06:22:15 UTC from IEEE Xplore. Restrictions apply.

Where $\mathbf{U}_S$ and $\mathbf{\Sigma}_S$ represent the signal subspace, and $\mathbf{U}_N$ and $\mathbf{\Sigma}_N$ represent the noise subspace.

During the subspace reconstruction process, the largest signal eigenvalue λ_1 and its corresponding eigenvector $\mathbf{w}_1$ are first removed, and the reconstructed subspace $\mathbf{\Phi}^1$ and the calibration matrix $\mathbf{Z}^1$ can be expressed as

$$\begin{aligned} \mathbf{\Phi}^1 &= \begin{bmatrix} \mathbf{w}_2 & \mathbf{w}_3 & \cdots & \mathbf{w}_{CS} \end{bmatrix}, \\ \mathbf{Z}^1 &= \operatorname{diag}\left[\lambda_2, \lambda_3, \cdots, \lambda_{CS}\right]. \end{aligned} \tag{15}$$

During the subspace reconstruction process, after the $(K-1)$-th iteration of removing the largest signal eigenvalue λ_{K-1} and its corresponding eigenvector $\mathbf{w}_{K-1}$, the reconstructed subspace and the calibration matrix can be given by

$$\begin{aligned} \mathbf{\Phi}^{K-1} &= \begin{bmatrix} \mathbf{w}_K & \mathbf{w}_{K-1} & \cdots & \mathbf{w}_{CS} \end{bmatrix}, \\ \mathbf{Z}^{K-1} &= \operatorname{diag}\left[\lambda_K, \lambda_{K+1}, \cdots, \lambda_{CS}\right]. \end{aligned} \tag{16}$$

By combining the reconstructed subspace spectrum function with the MUSIC algorithm, a set of reconstructed subspace spectrum estimation formulas can be represented as

$$\begin{cases} \mathbf{P}_s(\tau, f_d) = \frac{\mathbf{a}^H(\tau,f_d)\mathbf{U}_\mathrm{S}\mathbf{\Sigma}_\mathrm{S}^{-1}\mathbf{U}_\mathrm{S}^H\mathbf{a}(\tau,f_d)}{\mathbf{a}^H(\tau,f_d)\mathbf{U}_\mathrm{N}\mathbf{U}_\mathrm{N}^H\mathbf{a}(\tau,f_d)}, \\ \mathbf{P}^1(\tau, f_d) = \frac{\mathbf{a}^H(\tau,f_d)\mathbf{\Phi}^1\mathbf{Z}^1\mathbf{\Phi}^{1H}\mathbf{a}(\tau,f_d)}{\mathbf{a}^H(\tau,f_d)\mathbf{U}_N\mathbf{U}_N^H\mathbf{a}(\tau,f_d)}, \\ \vdots \\ \mathbf{P}^{K-1}(\tau, f_d) = \frac{\mathbf{a}^H(\tau,f_d)\mathbf{\Phi}^{K-1}\mathbf{Z}^{K-1}\mathbf{\Phi}^{K-1H}\mathbf{a}(\tau,f_d)}{\mathbf{a}^H(\tau,f_d)\mathbf{U}_N\mathbf{U}_N^H\mathbf{a}(\tau,f_d)}, \\ \mathbf{P}(\tau, f_d) = \frac{1}{\mathbf{a}^H(\tau,f_d)\mathbf{U}_N\mathbf{U}_N^H\mathbf{a}(\tau,f_d)}. \end{cases} \tag{17}$$

Accordingly, a new spatial spectrum estimation algorithm is obtained, the spectrum function of which is given by

$$\begin{aligned} \mathbf{P}(\tau, f_d) =& \mathbf{P}^1(\tau, f_d) \times \cdots \times \mathbf{P}^{K-1}(\tau, f_d) \times \\ & \mathbf{P}(\tau, f_d) \times \mathbf{P}_S(\tau, f_d). \end{aligned} \tag{18}$$

After peak search, the horizontal coordinate corresponding to the peak of the spectral function represents the time delay of the target's echo function to be estimated, while the vertical coordinate represents the Doppler frequency shift. Based on $d = \frac{c\tau}{2\Delta f}$ and $v = \frac{f_d c}{2 f_c T_s}$, the joint estimation of target's range and velocity can be performed.

C. PSO-RS-MUSIC Algorithm

The RS-MUSIC algorithm requires spectral peak searching in both the delay and Doppler frequency domains, which leads to high computational complexity, making it impractical for real-time estimation in ISAC systems. To solve this problem, the PSO-RS-MUSIC algorithm is proposed in this paper, which combines the PSO algorithm with RS-MUSIC. More specifically, the PSO algorithm can realize the spectral peak search in the delay-Doppler domain, which can significantly reduce computational complexity by replacing exhaustive grid searches with parallel optimization, while maintaining high-resolution parameter estimation. The particles adjust their movement based on their experience and the best solution found by the swarm, iterating to find the optimal range and velocity estimates with reduced computational complexity. This proposed algorithm can reduce computational complexity while ensuring accurate range and velocity estimation, thereby overcoming the inherent limitations of the RS-MUSIC algorithm.

The PSO aims to find the global optimal solution through iterative updates [14], [15]. Suppose the search space has D dimensions with the population size being M, during initialization, a population $S = \{s_1, s_2, \ldots, s_M\}$ consisting of M particles is randomly generated. Each particle's position is represented as a vector $\mathbf{s}_i = (s_{i1}, s_{i2}, \ldots, s_{iD})$, and its velocity as $\mathbf{v}_i = (v_{i1}, v_{i2}, \ldots, v_{iD})$. Each particle tracks its personal best position $P_{\text{best}} = (\mathbf{p}_{\text{best},1}, \ldots, \mathbf{p}_{\text{best,D}})$, which corresponds to the best solution found by the particle.

In the PSO algorithm, a swarm of G particles is randomly initialized, with each particle's position representing a candidate solution to the range-velocity estimation problem. These particles move in a 2-dimensional solution space, where one dimension corresponds to range and the other to velocity. Each particle's position is represented as a vector $\mathbf{s}_i = (s_{i1}, s_{i2})$, corresponding to a candidate pair of range and velocity values. The fitness of each particle is evaluated using the RS-MUSIC spatial spectrum based on the objective function $\mathbf{P}(\tau, f_d)$.

The fitness function is utilized to evaluate the quality of each particle's position in the solution space. During each iteration, the particle's current position is substituted into the fitness function, and its fitness value is calculated. By comparing the current fitness value with its historical best, the particle's personal best position P_{best} is updated if the current position results in a better fitness value. The global best position G_{best} is updated by comparing the fitness values of all particles in the swarm.

The velocity and position update equations are significant to the PSO algorithm, and the velocity update equation is given by

$$v_i^{k+1} = \omega v_i^k + c_1 r_1 (P_{\text{best}} - x_i^k) + c_2 r_2 (G_{\text{best}} - x_i^k), \tag{19}$$

where ω is the inertia weight, c_1 and c_2 are the learning factors, $r_1, r_2 \in [0, 1]$ are random numbers, x_i^k is the current position of particle i at iteration k, and p_{best} is the particle's personal best position. The position update equation is given by

$$x_i^{k+1} = x_i^k + v_i^{k+1}. \tag{20}$$

Through Eq.(19) and Eq.(20), the particles can gradually iterate and converge in the time-delay Doppler space until the stopping criteria are satisfied. This could be reaching a predefined number of iterations or when the fitness value of the global best position G_{best} converges, indicating that the particles have found a stable solution. Finally, the global best position G_{best} is output as the optimal solution for range and velocity estimation. The details of the proposed PSO-RS-MUSIC algorithm is summarized in **Algorithm 1**.

IV. Simulation Results

In this section, the estimation accuracy performance is presented to demonstrate the effectiveness of the proposed

Authorized licensed use limited to: BEIJING INSTITUTE OF TECHNOLOGY. Downloaded on July 09,2025 at 06:22:15 UTC from IEEE Xplore. Restrictions apply.

Algorithm 1 PSO-RS-MUSIC Algorithm for Joint Range-Velocity Estimation

Input: OFDM received signal $\mathbf{Z}$, segmentation (C, S), PSO parameters.
Output: Estimated range $\hat{d}$ and velocity $\hat{v}$.
Preprocessing:
Segment $\mathbf{Z}$ into submatrices $\mathbf{F}_{c,s}$ and form $\mathbf{R_d}$.
Subspace Construction:
Compute $\mathbf{R}_d$ and eigen-decompose.
Reconstruct subspaces $\{\Phi^i, \mathbf{Z}^i\}$.
PSO Search:
Initialize particles with random $(\tau^{(0)}, f_d^{(0)})$.
for $t = 1$ to T **do**
Evaluate fitness via $\mathbf{P}(\tau, f_d)$.
Update p_{best} and g_{best}.
Update velocities and positions.
end for
Estimation:
Extract $(\hat{\tau}, \hat{f}_d)$ from g_{best}.
Convert to $\hat{d} = \frac{c\hat{\tau}}{2\Delta f}$, $\hat{v} = \frac{c\hat{f}_d}{2f_c T_s}$.

algorithm. The basic parameters used in the simulation are summarized in Table I, and parameter setting strategies employed in the PSO algorithm is provided in Table II. A target to be estimated is set, with range and velocity parameters of $(50\,\text{m}, 50\,\text{m/s})$. The PSO-RS-MUSIC algorithm is applied to jointly estimate the range and velocity.

TABLE I: OFDM parameter settings

Symbol	Parameter	Value
f_c	Carrier frequency	3 GHz
Δf	Subcarrier spacing	50 kHz
N_c	Number of subcarriers	32
N_s	Number of evaluated symbols	32
B	Total signal bandwidth	1.6 MHz
T	Elementary OFDM symbol duration	20 μs
T_{CP}	Cyclic prefix duration	5 μs
T_s	OFDM symbol duration	25 μs

In [16], the optimal dimensions of the divided segmented matrix are given by

$$C = \left\lceil \frac{N_c}{3} \right\rceil, S = \left\lceil \frac{N_s}{3} \right\rceil. \tag{21}$$

TABLE II: Parameter settings for particle swarm optimization

Parameter	Value/Description
Population size (D)	50
Maximum iterations (T_m)	100
Inertia weight (ω)	0.7
Cognitive coefficient (c_1)	2.0
Social coefficient (c_2)	2.0

In Fig. 3, the performance of range and velocity estimation between the PSO-RS-MUSIC algorithm and the RS-MUSIC algorithm under different signal-to-noise ratio (SNR) conditions is presented. It can be observed that the estimation

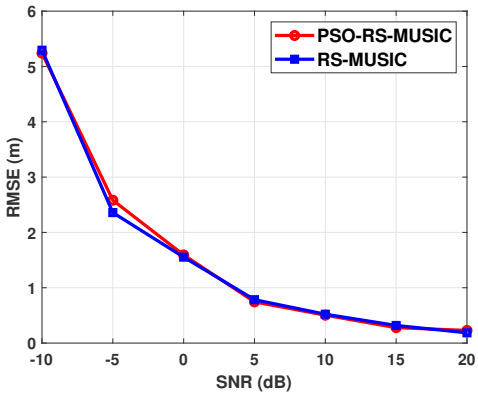

(a) The variation of range RMSE versus SNR.

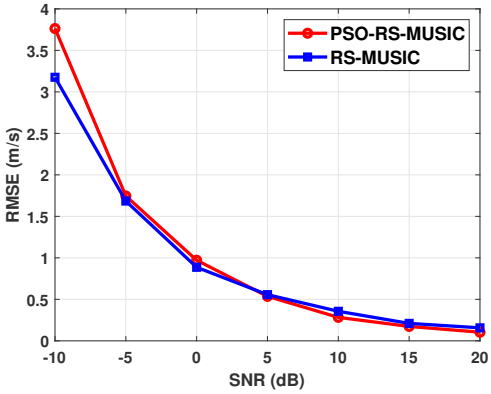

(b) The variation of velocity RMSE versus SNR.

Fig. 3: Range and velocity estimation performance of different algorithms under various SNRs.

performance of both algorithms improves as the SNR increases, and their estimation performances are almost identical in most cases. This indicates that both algorithms exhibit similar accuracy under high SNR conditions. Although the proposed method shows slightly reduced performance under low SNR conditions, such scenarios cannot be observed in practical systems.

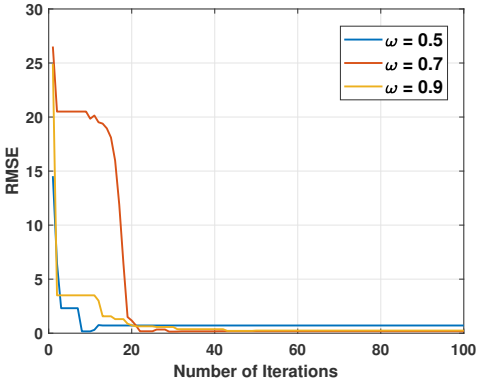

Fig. 4: Estimation performance of different ω values under various number of iterations.

Authorized licensed use limited to: BEIJING INSTITUTE OF TECHNOLOGY. Downloaded on July 09,2025 at 06:22:15 UTC from IEEE Xplore. Restrictions apply.

Fig. 4 shows the RMSE variation of the PSO-RS-MUSIC algorithm under different inertia weights. It can be observed that the RMSE values for all inertia weights are relatively high in the initial stage, indicating a high level of randomness in particle initialization. The performance of the PSO algorithm varies under different inertia weights. When $\omega = 0.7$, the RMSE decreases the fastest, indicating that the PSO algorithm achieves a better balance between global exploration and local exploitation. After about 30 iterations, the RMSE stabilizes for all inertia weights, suggesting that the PSO-RS-MUSIC algorithm converges to an optimal or near-optimal solution. Overall, the inertia weight significantly impacts the performance of the PSO-RS-MUSIC algorithm, with $\omega = 0.7$ demonstrating the best performance in terms of convergence velocity and accuracy.

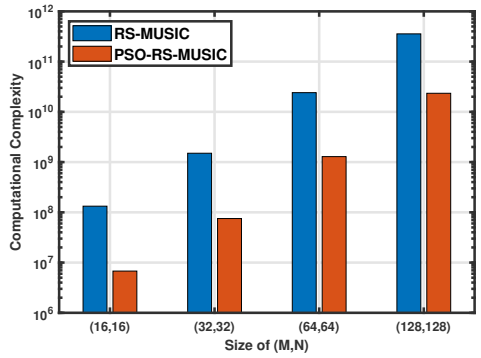

Fig. 5: Computational complexity of different algorithms.

The computational complexity of the RS-MUSIC algorithm for radar ranging and velocity measurement is analyzed below. First, the computational complexity of the covariance matrix calculation is $CS(N_c - C)(N_s - S)$ complex multiplications. The eigenvalue decomposition of the covariance matrix requires C^3S^3 complex multiplications. The two-dimensional peak search requires $J_1J_2(CS + 1)(CS - K)$ complex multiplications. Therefore, the total computational complexity is $O(CS(N_c-C)(N_s-S)+C^3S^3+J_1J_2(CS+1)(CS-K))$,where J_1J_2 represents the search lengths in the dimensions of range and velocity. In contrast, the complexity of the PSO-RS-MUSIC algorithm is significantly reduced, and the complexity of its two-dimensional peak search is $T_mN_s((CS + 1)(CS - K) + D)$, therefore, the total computational complexity is $O(CS(N_c - C)(N_s - S) + C^3S^3 + T_mN_s((CS+1)(CS-K)+D))$. In the design of this simulation experiment, the PSO peak search reduces the algorithm's complexity by more than 90%. As shown in the Fig 5, the PSO-RS-MUSIC algorithm demonstrates a marked reduction in complexity across all matrix sizes, particularly for smaller matrices like (16,16) and (32,32). This efficiency improvement is benefitted from PSO's ability to optimize the peak search process, which reduces the number of iterations required, thus making the algorithm more suitable for real-time applications where fast processing is essential.

V. Conclusions

In this paper, the PSO-RS-MUSIC algorithm was proposed as a low-complexity solution for joint range and velocity estimation in ISAC systems. To improve the estimation accuracy, an optimized subspace reuse mechanism was proposed. Moreover, to further reduce the computational complexity, particle swarm optimization was utilized to find the peak instead of traditional spectral peak search. Simulation results show that comparable performance to the RS-MUSIC algorithm can be achieved, while complexity is significantly reduced, which shows the effectiveness of the proposed range and velocity joint estimation in terms of both accuracy and efficiency.

Acknowledgments

This work was supported in part by the National Key Research and Development Program of China under Grant 2024YFE0200404.

References

[1] F. Liu *et al.*, "Integrated sensing and communications: Toward dual-functional wireless networks for 6G and beyond," *IEEE J. Sel. Areas Commun.*, vol. 40, no. 6, pp. 1728-1767, Jun. 2022.

[2] T. Yang *et al.*, "A Unified Tensor-Based Joint AUD and ISAC Parameter Estimation With Large-Scale User Access," *IEEE Trans. Cognit. Commun. Networking*, early access, Feb. 25, 2025, doi: 10.1109/TCCN.2025.3545690.

[3] N. Wu *et al.*, "AI-Enhanced Integrated Sensing and Communications: Advancements, Challenges, and Prospects," *IEEE Communications Magazine*, vol. 62, no. 9, pp. 144–150, 2024.

[4] L. Mai, J. Yao, and Q. Zhang, "Joint state sensing and communication systems with OFDM transmission," *IEEE Commun. Lett.*, vol. 27, no. 11, pp. 2948-2952, Nov. 2023

[5] F. Zhang *et al.*, "Joint range and velocity estimation with intrapulse and intersubcarrier Doppler effects for OFDM-based RadCom systems," *IEEE Trans. Signal Process.*, vol. 68, pp. 662-675, 2020.

[6] X. Tian *et al.*, "Range and velocity estimation for OFDM-based radar-radio systems," in *Proc. WCSP*, Nanjing, China, 2017, pp. 1-6.

[7] Y. Xiang, Y. Gao, X. Yang, S. Kang, and M. Shao, "An ESPRIT-based moving target sensing method for MIMO-OFDM ISAC systems," *IEEE Commun. Lett.*, vol. 27, no. 12, pp. 3205-3209, Dec. 2023.

[8] R. Bomfin and M. Chafii, "Unique word-based frame design for bistatic integrated sensing and communication," *IEEE Trans. Wireless Commun.*, vol. 23, no. 12, pp. 19333-19349, Dec. 2024.

[9] A. Chowdary, A. Bazzi, and M. Chafii, "On hybrid radar fusion for integrated sensing and communication," *IEEE Trans. Wireless Commun.*, vol. 23, no. 8, pp. 8984-9000, Aug. 2024.

[10] X. Wang *et al.*, "Range and velocity estimation for multi-symbol OFDM-based integrated radar and communications systems," in *Proc. IEEE CIE Int. Conf. Radar (ICR)*, Haikou, China, 2021, pp. 2457-2460.

[11] Z. Wang *et al.*, "Joint angle and range estimation with two-level nested FDA-MIMO radar," in *Proc. ICICSP*, Xi'an, China, 2023, pp. 1023-1027.

[12] N. Ahmed *et al.*, "Performance analysis of efficient computing techniques for direction of arrival estimation of underwater multi targets," *IEEE Access*, vol. 9, pp. 33284-33298, 2021.

[13] J. P. Merkofer *et al.*, "DA-MUSIC: Data-driven DoA estimation via deep augmented MUSIC algorithm," *IEEE Trans. Veh. Technol.*, vol. 73, no. 2, pp. 2771-2785, Feb. 2024.

[14] M. Li and Y. Lu, "Maximum likelihood DOA estimation in unknown colored noise fields," *IEEE Trans. Aerospace Electron. Syst.*, vol. 44, no. 3, pp. 1079-1090, Jul. 2008.

[15] W. Zhang and W. Zhang, "An efficient UAV localization technique based on particle swarm optimization," *IEEE Trans. Veh. Technol.*, vol. 71, no. 9, pp. 9544-9557, Sept. 2022.

[16] R. Xie *et al.*, "Performance analysis of joint range-velocity estimator with 2D-MUSIC in OFDM radar," *IEEE Trans. Signal Process.*, vol. 69, pp. 4787-4800, 2021.

Authorized licensed use limited to: BEIJING INSTITUTE OF TECHNOLOGY. Downloaded on July 09,2025 at 06:22:15 UTC from IEEE Xplore. Restrictions apply.